

Genetic and Immunological Evidence for Microbial Transfer Between the International Space Station and an Astronaut

David C. Danko^{1,2}, Nitin Singh³, Daniel J. Butler², Christopher Mozsary², Peng Jiang⁴, Ali Keshavarzian⁵, Mark Maienschein-Cline⁴, George Chlipala⁴, Ebrahim Afshinnkoo², Daniela Bezdán², Francine Garrett-Bakelman^{2, 6, 7}, Stefan J. Green⁴, Fred W. Turek⁸, Martha Hotz Vitaterna⁸, Kasthuri Venkateswaran³, and Christopher E. Mason^{2,10,*}

¹Tri-Institutional Computational Biology & Medicine Program, Cornell University, NY, USA

²Institute for Computational Biomedicine, Department of Physiology and Biophysics, Weill Cornell Medicine of Cornell University, NY, USA

³Biotechnology and Planetary Protection Group, Jet Propulsion Laboratory, California Institute of Technology, Pasadena, Los Angeles, CA

⁴University of Illinois at Chicago, Chicago, IL, USA

⁵Rush University Medical Center, Chicago, IL USA

⁶Department of Medicine, University of Virginia, Charlottesville, VA

⁷Department of Biochemistry and Molecular Genetics, University of Virginia, Charlottesville, VA

⁸Northwestern University, Evanston, IL, USA

⁹The Feil Family Brain and Mind Research Institute, Weill Cornell Medicine, NY, USA

*Corresponding author

Abstract

Microbial transfer from the environment can influence a person's health, but relevant studies often have confounding variables and short durations. Here, we used the unique environment of the International Space Station (ISS) to track movement of microbes between an astronaut's commensal microbiomes and their environment. We identified several microbial taxa, including *Serratia proteamaculans* and *Rickettsia australis* which appear to have been transferred from the ISS to the commensal microbiomes of the astronaut. Strains were matched at the SNP and haplotype-level, and notably some strains persisted even after the astronaut's return to Earth. Some transferred taxa correspond to secondary strains in the ISS environment, suggesting that transfer may be mediated by evolutionary selection. Finally, we show evidence that the T-Cell repertoire of the astronaut changes to become more specific to environmental taxa, suggesting that continual microbial and immune monitoring can help guide spaceflight mission planning, health monitoring, and habitat design.

Keywords: microbiome, twin-study, spaceflight, microbial transfer, immunology, t-cell

1 Introduction

Human commensal microbiomes have a known hereditary component (Goodrich et al., 2016), but the non-hereditary, acquired portion of the human microbiome is still being defined in terms of its covariates and components. It is known that the microbiome can change as a function of age, diet, developmental stage, environmental exposures, antibiotic use, and lifestyle, yet strain-level mapping and longitudinal tracking of such dynamics are limited. In particular, the movement of non-pathogenic microbes and how they can colonize an adult commensal microbiome in a defined, quantified, and sealed environment, is almost completely unknown (Schwendner et al., 2017). An ideal study for microbial transfer would utilize a longitudinal sampling of subjects in a hermetically-sealed environment that was already profiled with strain-level resolution.

As an environment, the International Space Station (ISS) presents several key advantages for the study of microbial transfer. It is a well studied environment, with microbial tracking studies ongoing since 2014, and its occupants' microbiomes are routinely sequenced. Moreover, the ISS is a uniquely sealed environment with essentially no chance of infiltration by exterior microbes, save for the regular supply missions. Finally, microgravity on the ISS may lead to an improved diffusion of microorganisms relative to studies done in terrestrial environments.

30 Evidence for the transfer environmental microbes into adult commensal microbiomes could have
31 important health implications, as it would provide a mechanism for how regional environmental micro-
32 biomes impact a person’s microbiome. Cities in particular are known to host diverse environmental
33 microbiomes (Danko et al., 2019) and transfer between commensal and environmental microbiomes may
34 add to explanations for health differences between otherwise similar regions (Nicolaou et al., 2005). The
35 selective transfer of certain microbial strains may also carry evolutionary implications for the microbes
36 being transferred. If a microbial species can be shown to follow distinct selective patterns inside and
37 outside of human commensal microbiomes, or even on the ISS, it is possible that these patterns could
38 guide strain or even species differentiation.

39 Here, we present genetic and immunological evidence for the transfer of environmental strains to an
40 astronaut’s gut and oral microbiome while on the International Space Station (ISS) during an almost
41 year-long mission (Garrett-Bakelman et al., 2019a). The strain-level data was compared to the T-cell
42 receptor (TCR) diversity and sequence changes during the mission, and these increased matches mid-
43 flight corresponded to the candidate microbial strains observed. Of note, several of these strains were
44 still observed for months after the mission, providing evidence of a persistent influence on the astronaut’s
45 microbiome, which may help to inform future studies on human microbial interaction.

46 2 Results

47 We collected 18 fecal and 23 oral microbiome samples from two identical twin human astronauts, one
48 flight subject (TW, 9 stool, 6 saliva, 5 buccal) and one control who did not leave Earth (HR, 9 stool,
49 7 saliva, 5 buccal), taken from 2014-2018. These were compared to 42 time-matched, environmental
50 samples from the ISS that corresponded to the flight subject’s mission duration. All samples were
51 sequenced with 2x150bp read length to a mean depth of 12-15M reads (12.01, 14.96, and 14.97M mean
52 reads for ISS, fecal, and saliva, respectively), then aligned to the catalog of NCBI RefSeq complete
53 microbial genomes, examined for single nucleotide polymorphisms (SNPs), and then run with strain
54 analysis with the MetaSUB CAP pipeline and Aldex2 (see Methods).

55 2.1 Taxonomic profiles show evidence of continual microbial exchange

56 **New taxa in flight subject (TW) match environmental and commensal microbiomes** We
57 first examined the proportion of taxa observed in a given sample that were not observed in a previous
58 sample from the same donor. Any newly observed taxa in sample of a given type (e.g. stool) was
59 annotated relative its presence in samples from other body or environmental sites (e.g saliva). For fecal
60 samples, we segmented the previously unobserved taxa from each sample into four groups: taxa observed
61 in any saliva sample taken before the given fecal samples, taxa observed in ISS samples but not observed
62 in saliva, taxa observed in both ISS and saliva samples, and taxa that were not observed in either the
63 ISS or the saliva. The same process was repeated for saliva samples but swapping fecal and saliva in the
64 hierarchy. As expected, the time series of samples taken from the flight subject (TW) and ground control
65 subject (HR) showed that earlier samples exhibited a greater proportion of novel organisms (Figure 1,
66 S1).

67 Of note, each sample contains a number of unobserved taxa that matched taxa from saliva/feces
68 or the ISS (even before flight), indicating these are common commensal species on Earth or possibly
69 organisms absorbed in previous missions. Indeed, both astronauts had previously been in the space
70 station across multiple missions though with a 10-fold difference in duration (TW has logged 520 total
71 days on the ISS vs. 54 days for HR). Interestingly, when we examined the fraction of taxa that match
72 ISS taxa in pre-flight samples from TW compared to other samples from HR, a higher average rate (
73 56%) of ISS-matching taxa was observed in pre-flight samples for TW relative to HR (51%), although
74 not significant (p-value = 0.21). The fraction of taxa that matched different environments are listed in
75 Table 1. For both saliva and fecal microbiomes, the large majority of taxa at each time point had already
76 been observed in a previous sample from that site.

77 A small number of taxa were never observed in any pre-flight sample from any body site from either
78 HR or TW, but were observed in mid- and post-flight samples from TW. We thus filtered for taxa that
79 had no reads observed in pre-flight samples and had at least ten reads in at least two mid- or post-flight
80 samples. These taxa were further filtered for taxa that were observed in at least two ISS samples. The
81 resulting list included five taxa: two viral genera, two viral species (both phage), and one bacterial
82 species: *Rickettsia australis* (Figure 2). Given the generally low abundance of these taxa, we cannot

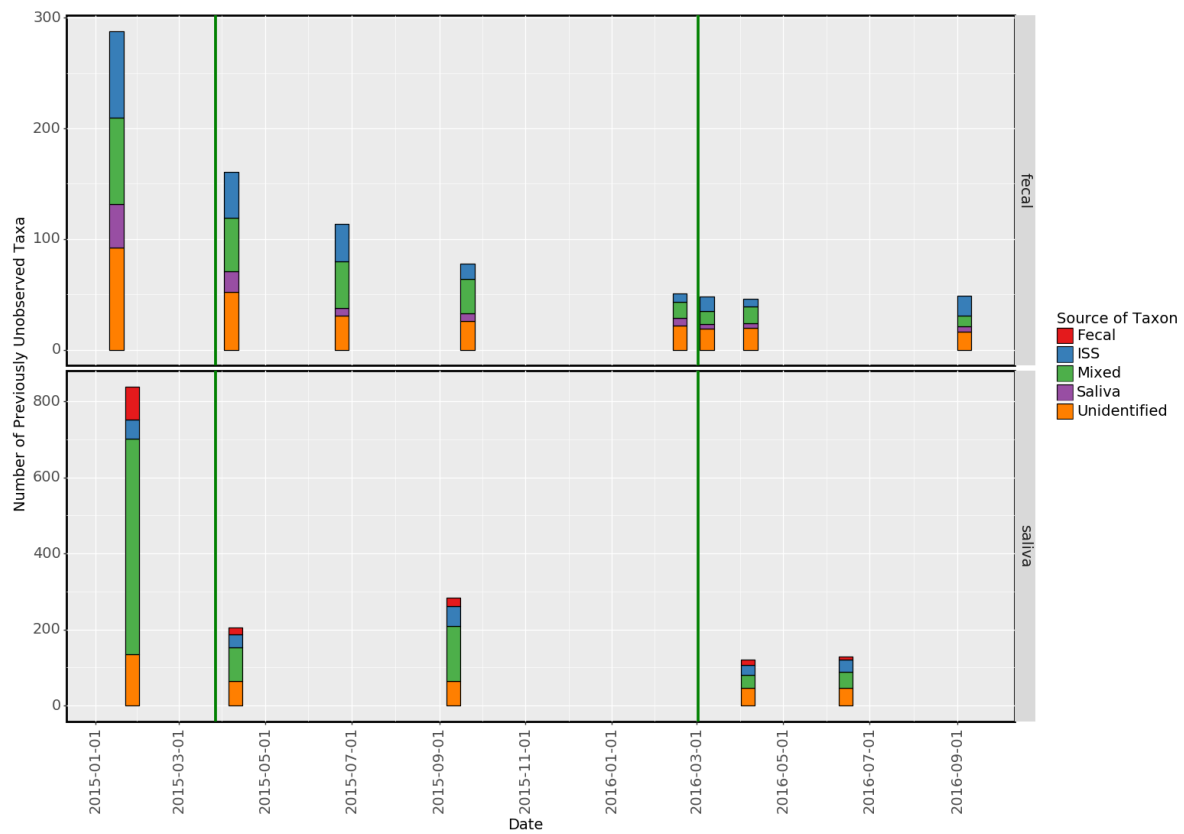


Figure 1: This plot shows the number of taxa at each time point that were not observed at any previous timepoint for fecal and saliva samples from TW. The colors indicate the likely source of the new taxon if it was found previously in the saliva (for fecal samples, vice versa for saliva samples), the ISS, both (Mixed), or neither.

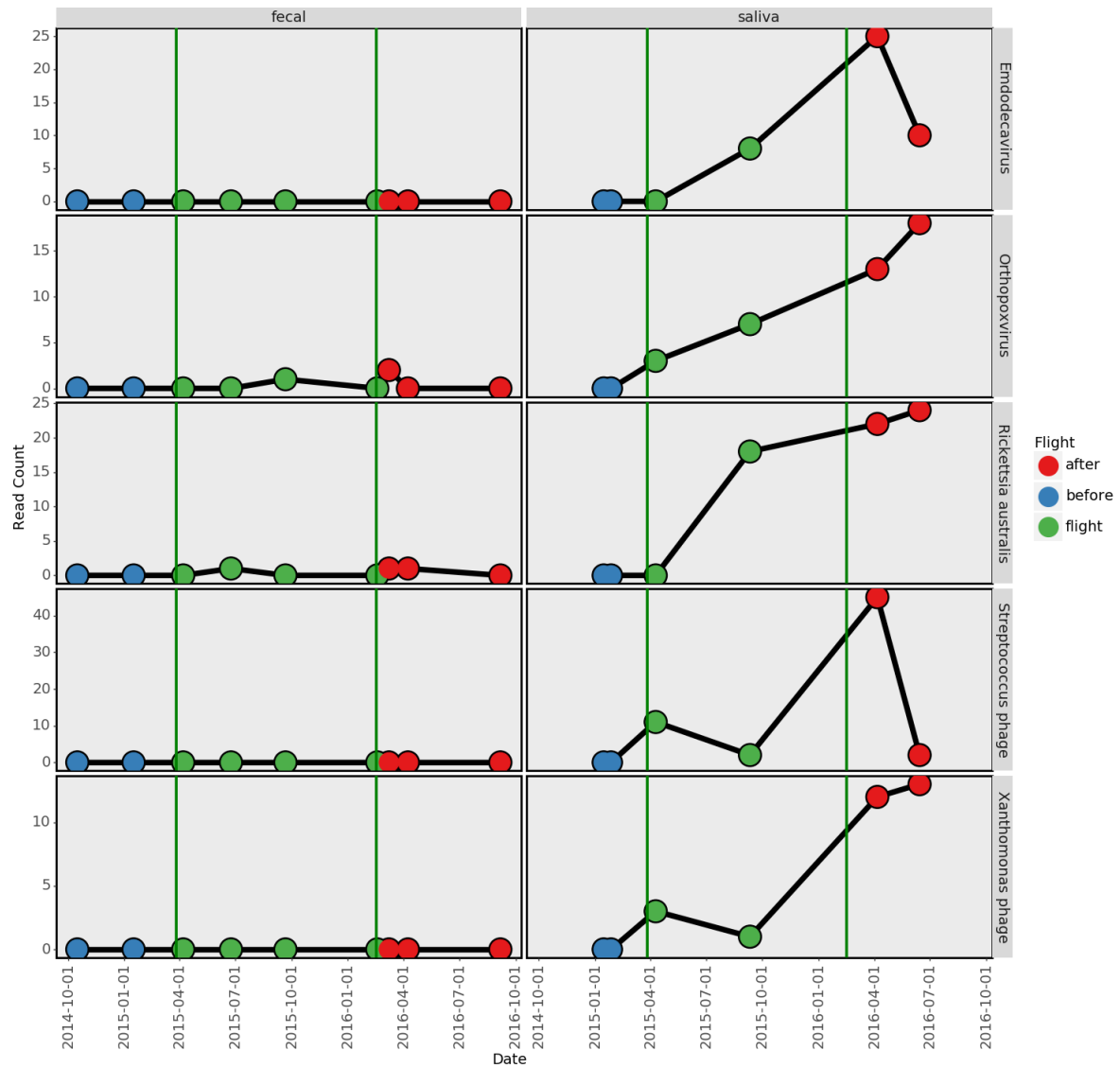


Figure 2: Total number of reads observed in TW for different taxa not observed before flight. Green vertical bars indicate the start and end of flight. The *Streptococcus phage* referenced is *phiARI0004*, *Xanthomonas phage* is *vB XveM DIBBI*,

83 definitively rule out that they were present at an undetectable, low threshold pre-flight, but our data
84 show no reads supporting their presence.

85 **Emergence of new taxa in gut microbiomes exceeds repeated sampling** To place these tax-
86 onomic trends in context, we investigated whether the sampling time series from TW and HR would
87 identify more new taxa than repeated assays on an unchanging fecal sample. We compared the fecal
88 microbiome time series of TW and HR to 243 repeated samples taken from a single fecal sample ([Sasada
89 et al., 2020](#)), using 100,000 random sets of 9 samples (to match the twins' set size). The number of
90 taxa in each sample that had not been observed in any previous sample were counted for each subset
91 and normalized by the total number of taxa in the first sample. The time series for HR showed signifi-
92 cantly more new taxa than 99,971 ($p = 2.9e-4$) random stool subsets, and TW was even more significant
93 (more than 99,990, $p = 1.0e-4$) relative to random subsets (Figure 3). These results shows that the time
94 series for TW and HR both consistently had more taxa than would be expected from re-sampling an
95 unchanged fecal sample. Differences between TW and HR may have a large number of causes including:
96 diet, environment, and exposure to other people. For our subsequent analysis, it is relevant that both
97 TW and HR show more new taxa than re-sampling a single sample, since it implies transmission may
98 be occurring (possible for both subjects though we do not have data on HR's environment for direct
99 comparison).

100 **Evidence of higher transfer rates on board the ISS** To characterize this possible microbial
101 exchange, we next calculated taxonomic diversity using Shannon's entropy for species profiles of each
102 sample (Figure S2). For both fecal and saliva samples from TW, the highest diversity was observed
103 during flight, and this trend was not observed for HR in the same time intervals. However, given
104 the small sample size this trend was not significant ($p=0.21$). Nonetheless, we identified a significant
105 increase in the number of previously unobserved taxa for samples taken from TW during flight (Figure
106 S3) compared to random permutations.

107 To further characterize the significance of such transfer relative to the sampling set and the source,
108 we performed a series of permutation tests. We first established the number of previously unobserved
109 species found at each time point in the actual data from TW. We then randomly shuffled and relabeled
110 these samples and counted species again for a total of 10,000 random permutations. We then counted
111 the number of permutations where the number of species observed 'during flight' in the shuffled data was
112 higher than the real data. For the fecal microbiome the actual number of observed taxa was higher than
113 the shuffled data in 96.7% of cases, for saliva 98.2% of cases and for buccal the observed was higher than
114 all other permutations. Repeating the same procedure on data from HR ('flight' status was arbitrarily
115 assigned to the second, third, and fourth samples) we observed 45.9% for feces 98.2% for saliva, and
116 80.1% for buccal (more buccal samples were available for HR).

117 Results were similar when the above procedure was repeated only with taxa found in ISS environmen-
118 tal samples (TW fecal 97.5%, TW saliva 97.7%, TW buccal all permutations, HR fecal 33.6%, HR saliva
119 98.3%, HR buccal 81.1%). An analogous analysis performed on ISS samples (Figure S4) showed that
120 microbial data during TW's flight did not have significantly more new taxa than shuffled time periods
121 (higher than 557 of 1,000 permutations). This is expected since the ISS is under continual habitation
122 and merely is meant to show the converse of HR as a second control.

Table 1: This table gives the average percent overlap between the number of emergent taxa in fecal and saliva microbiomes and microbiomes in other sites.

Commensal Type	Fecal	Saliva
Sites Where Taxa Originated		
Fecal Only	n/a	8.7
Saliva Only	10.2	n/a
ISS Only	24.5	17.6
Both ISS & Saliva/Fecal	29.9	44.6
Taxa not identified in another site	35.5	29.1

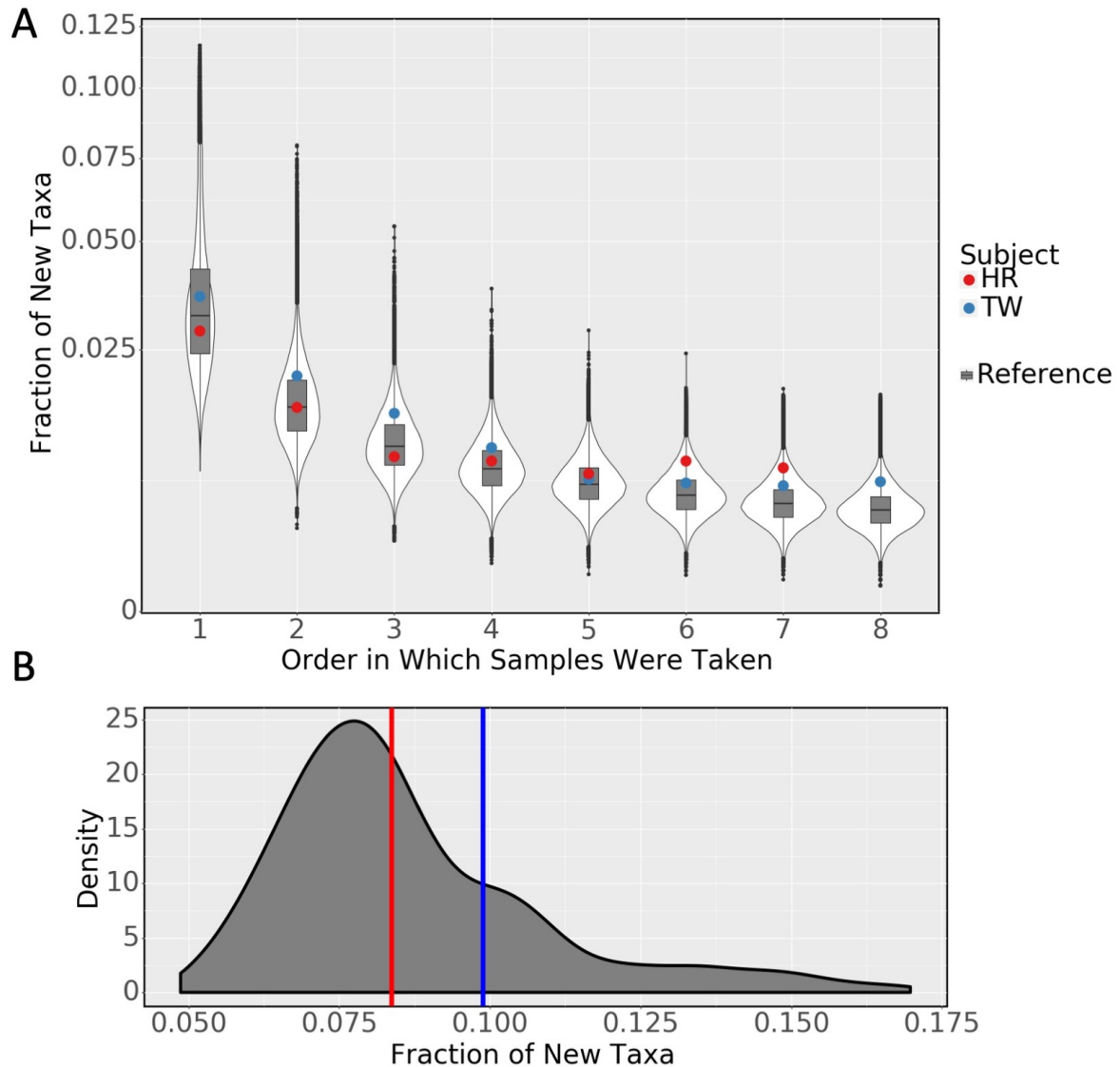


Figure 3: A) The number of new taxa observed in TW and HR are higher than repeated resampling of the same fecal sample. The y-axis gives the number of new taxa at each time point (not observed at any previous time point) divided by the number of taxa in the first sample. The first time point is omitted from the plot because it is always 1 by construction. The x-axis gives the order of each sample (arbitrary for random subsample). Boxplots show the distribution of random subsamples. Colored points are the actual time series. B) The number of unique taxa observed after the first time point divided by the number of taxa at the first time point. Same legend as (A)

123 2.2 Strain level variation confirms microbial transfer

124 **Novel genome regions in flight found in environmental and commensal microbiomes** Given
125 the higher overall transfer rate of species on the ISS, we next examined the strain emergence and persis-
126 tence (post-flight) of such species. We selected a set of candidate taxa that showed significantly greater
127 abundance during and after flight in TW compared to pre-flight, and then mapped reads to known ref-
128 erence genomes from these taxa. We looked at the coverage of reference genomes in samples from TW
129 at each stage of flight (concatenating samples from the same stage) and in the ISS and grouped regions
130 into three categories: regions which were covered before flight, regions that were covered before flight in
131 either gut or saliva samples but not observed in the other until flight, and regions that were not observed
132 in either gut or saliva samples until flight but were found in the ISS environment. Example coverage
133 plots are shown for two taxa: *Fusobacterium necrophorum* and *Serratia proteamaculans* (Figure S5 and
134 Figure S6B respectively). The total size of these genomic regions for all tested taxa are listed in Table 2.

135 For the selected taxa, the average environmental transfer of genomic regions were 32.2% of the size of
136 pre-flight regions, whereas gut-saliva transfers were lower at 19.9%. The taxa with the (proportionally)
137 largest transferred regions *Cronobacter condimenti*, had 55.9% gut-saliva transfer and 123.7% environ-
138 mental transfer. The presence of (in some taxa) large genomic regions that were not covered until flight
139 strongly suggests that individual species are undergoing flux with new strains and genes migrating into
140 commensal microbiomes and/or a greater abundance of the strain.

141 **Microbial SNPs match environmental and commensal microbiomes** Once the candidate ge-
142 nomic regions were identified, we next mapped co-occurring clusters of SNPs (haplotypes) in the selected
143 taxa listed above in all samples from TW, HR, and the ISS (Figure 4). We matched microbial haplotypes
144 from TW during flight to possible sources in pre-flight TW samples and ISS samples. We considered
145 five groups as potential sources for haplotypes in mid-flight fecal samples: haplotypes found in pre-flight
146 fecal samples, haplotypes found in pre-flight saliva but not fecal or ISS samples, haplotypes found in
147 the ISS but neither saliva nor fecal, haplotypes found in both the ISS and saliva (mixed) but not fecal,
148 and haplotypes not observed in any other group. For saliva samples we used the same five groups but
149 replaced fecal with saliva and vice versa.

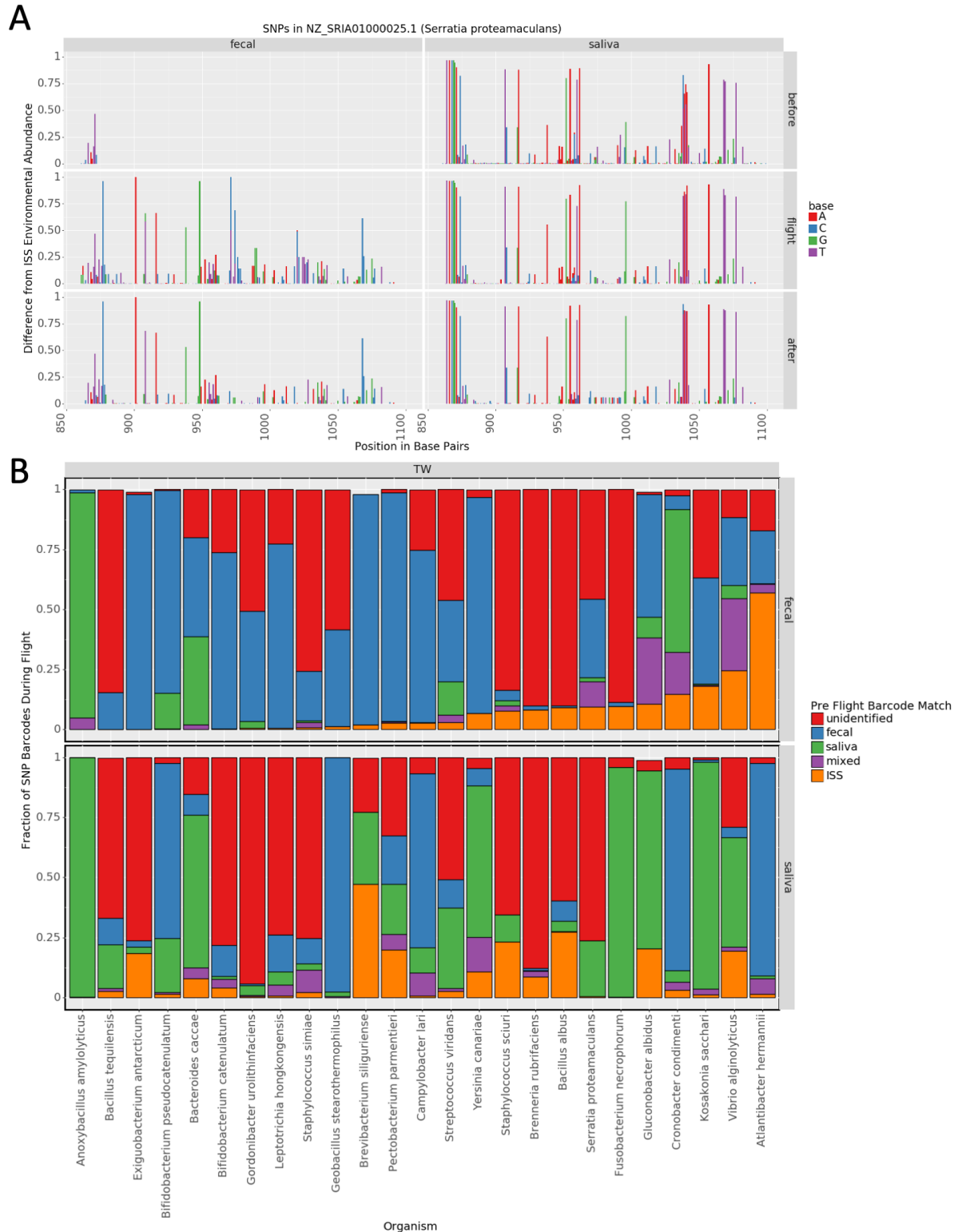
150 The pre-flight sources of haplotypes varied by the species being investigated (Figure 4B). Some species,
151 such as *Cronobacter condimenti* showed an apparent flip of strains from the gut microbiome to saliva and
152 vice versa. Other taxa, like *Atlantibacter hermannii*, showed a large fraction of haplotypes that matched
153 environmental haplotypes in the gut microbiome. Some taxa, like *Bifidobacterium catenulatum* showed
154 little similarity to any potential external source.

155 2.3 Transfer of *Serratia proteamaculans*

156 ***Serratia proteamaculans* (SP) is a candidate of persistent transfer** We identified *S. protea-*
157 *maculans* as a candidate species for persistent transfer, since it was found in ISS environmental samples
158 and was significantly more abundant in mid- and post flight fecal samples from TW than in fecal samples
159 from TW pre-flight and HR samples. Overall, *S. proteamaculans* was only found at low levels in fecal
160 samples in TW pre-flight, was significantly more abundant during flight, and dropped to an intermediate
161 level after flight (Figure S6A). No major variation in abundance was observed for the control twin HR.
162 SP was roughly uniformly abundant in the saliva before during and after flight.

163 **Regions of the SP genome are found in TW fecal samples only after arrival at the ISS** We
164 identified regions of the SP genome which appeared in fecal samples after TW was on board the ISS. We
165 found three such regions totaling about 1.5kbp. The abundance of these regions roughly matched the
166 overall pattern seen for *S. proteamaculans*: very low or undetectable pre-flight, a high during flight, and
167 an intermediate level post flight (Figure S6B). These regions were all well covered from ISS environmental
168 samples.

169 Total coverage of the SP genome in TW from all available fecal samples was 29.2kbp. Before flight
170 8.9kbp was covered, during 17.2kbp and after 19.0kbp. However some of these regions were either quite
171 small or not covered in both mid- and post flight. As, such 1.5kbp represents a reasonable fraction of
172 the amount of SP genome covered in TW but should only be interpreted as evidence for the transfer of
173 particular genes.



174 **SNPs in post-arrival regions match a secondary environmental strain** We next analyzed one
175 of the above regions (of about 250bp) for SNPs (Figure 4A) and identified SNPs in samples from TW
176 which did not match the dominant strain in the ISS environment. We identified 9 such SNPs in this
177 region in fecal samples taken from TW during flight. Of these 9 SNPs, 6 were also found after the
178 conclusion of flight. No SNPs were found in fecal samples from TW before flight owing to the fact that
179 no reads mapped to this region. We note that all 9 SNPs were found in the ISS environment at some
180 proportion and that this region did not match any other reference genome in RefSeq besides SP.

181 Next we sought to determine if these 9 SNPs could have come from a secondary strain on the ISS.
182 We used the SNP clustering technique described in the methods to determine if the 9 SNPs we identified
183 could have come from the same underlying sequence. We identified corresponding barcodes (groups of
184 co-stranded SNPs) of 8 SNPs in TW and 9 SNPs in the ISS environment. The groups in TW included 8
185 out of the 9 mid-flight SNPs. The 9 SNP group from the ISS environment included these same 8 SNPs
186 as well as one SNP not identified in TW. This leads us to the conclusion that the strain found in TW
187 likely represented a secondary strain in the ISS environment.

188 Finally, we checked if the strain could have come from TW's oral microbiome. The region in question
189 was covered by reads in the oral microbiome before flight. However, when we performed the same analysis
190 as above using reads from TW's oral microbiome we found a distinct SNP pattern (Figure 4A) giving
191 evidence that the strain found in flight likely did not come from the oral microbiome.

192 **2.4 Changes to immune repertoire in flight suggest environmental transfer**

193 **Immune repertoire in TW changes during flight** We surveyed the alpha (intra-sample) and beta
194 (inter-sample) diversity for the repertoires of T-Cell Exposed Motifs (TCEMs) found in each sample
195 from RNA-sequencing of CD4+ sorted peripheral blood mononuclear cells (PBMCs) from TW and HR
196 (Garrett-Bakelman, 2019). To assess beta diversity we performed a UMAP dimensionality reduction using
197 Manhattan distance between the TCEM repertoires (with abundance) from each sample. As expected,
198 there was little similarity between the three types of TCEM motifs (types 1, 2a, and 2b Figure S7).
199 Within each type of motif, there was weak clustering between the different stages of flight for TW and
200 overlap with HR (Figure 5A). This indicates a possible shift during flight. The clustering does not seem
201 to be due to a batch effect from the return of 3 flight samples directly from the ISS, as these samples
202 cluster more closely with fresh frozen samples than they do with the ambient return sample from HR
203 (Figure S8).

204 We next assessed alpha diversity by randomly subsetting TCEM repertoires from each sample to
205 5,000 total TCEMs (fewer unique TCEMs as the same sequence could be taken multiple times) and
206 taking Shannon's Entropy ($H = -\sum_i p_i \log_2(p_i)$) of each sample (Figure 5B). Shannon's entropy was used
207 because it accounts for differences in abundance. We observed a large drop in diversity in TW during
208 flight which partially recovered after flight. By comparison, the TCEM profile for HR was relatively
209 stable (10.8-11.1).

210 **TCEMs match environmental targets in the ISS** We next compared the overlap of TCEM
211 repertoires in each sample to potential TCEM targets in ISS environmental samples. All PMA treated
212 samples (to select for intact cell membranes, and likely bacterial viability) from the ISS during TWs
213 flights were pooled. We produced a set of potential TCEM targets and filtered all targets that occurred
214 in less than one part per million. This left a set of 176,204 potential environmental TCEM targets. We
215 found the fraction of TCEMs (of all types) that occurred in the set of potential targets for each time
216 sample from TW and HR. The fraction of TCEMs that overlapped with ISS targets increased in TW
217 during flight (Figure 6A) and returned to an intermediate level after flight, and was the highest at the
218 later points of the year-long mission. No corresponding change was observed in samples from HR.

219 For further comparison, we took the anti-sense protein (as described in Root-Bernstein (2016)) of
220 each TCEM and compared the set of anti-TCEMs for each sample to the environmental targets. The
221 anti-sense protein has no clear biological significance for TCEMs so this was meant as a negative control.
222 As expected there was no clear pattern in the overlap between anti-TCEMs and environmental targets
223 (Figure S9).

224 **Taxa found in the ISS are enriched for sequences that match TCEMs in TW during flight**
225 We next identified taxa that contained proteins which matched the sequences for TCEMs. Since TCEMs
226 are just 5 amino acids long and can match many different taxa, we pooled TCEM repertoires from flight
227 and pre-flight samples from TW and found matching taxa for all TCEMs in the pooled repertoires.

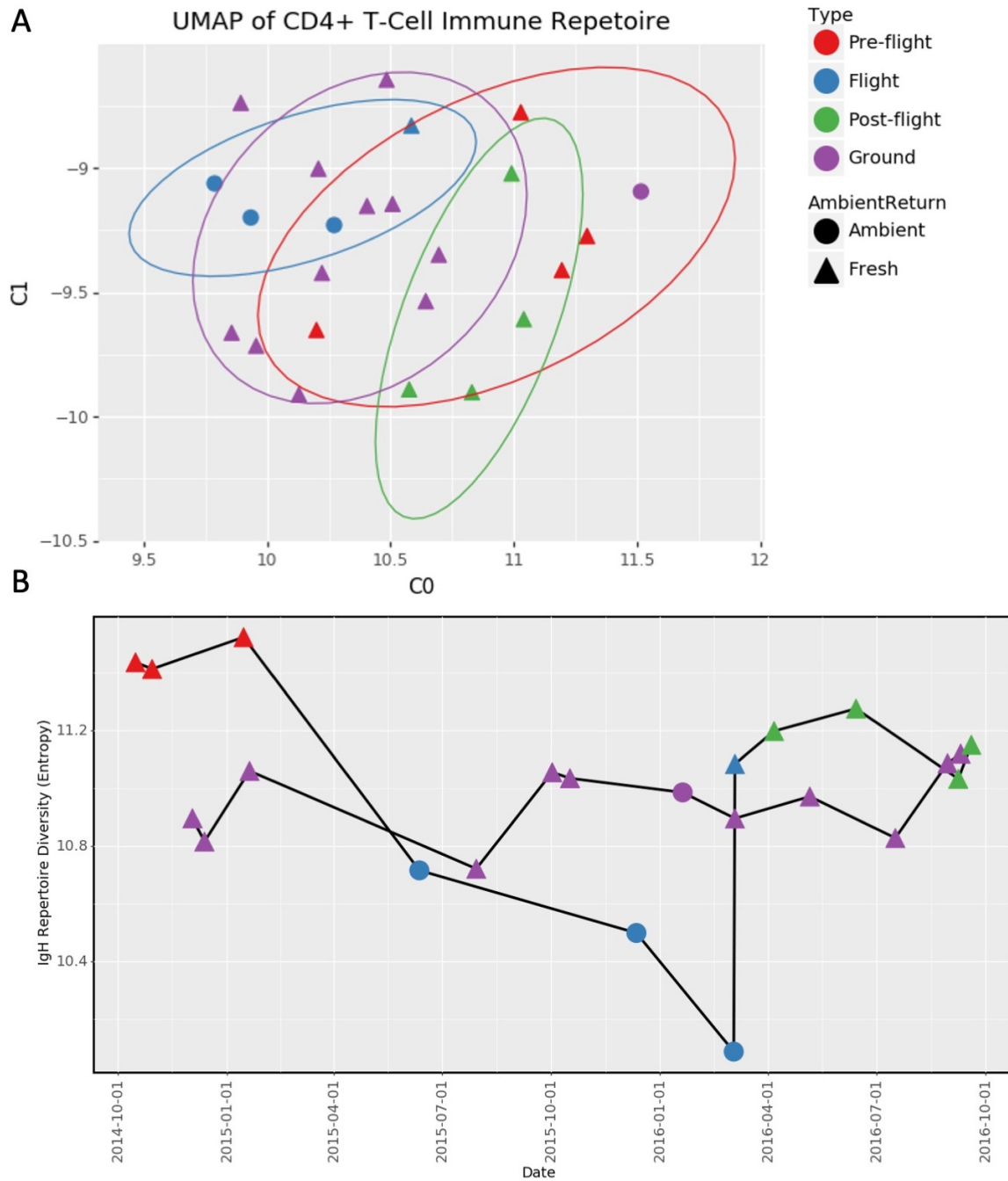


Figure 5: A) UMAP plot of similarity between Type 1 TCEM repertoires. B) Entropy of depth normalized TCEM repertoires. Legened is the same for both panels, 'Ground' indicates HR.

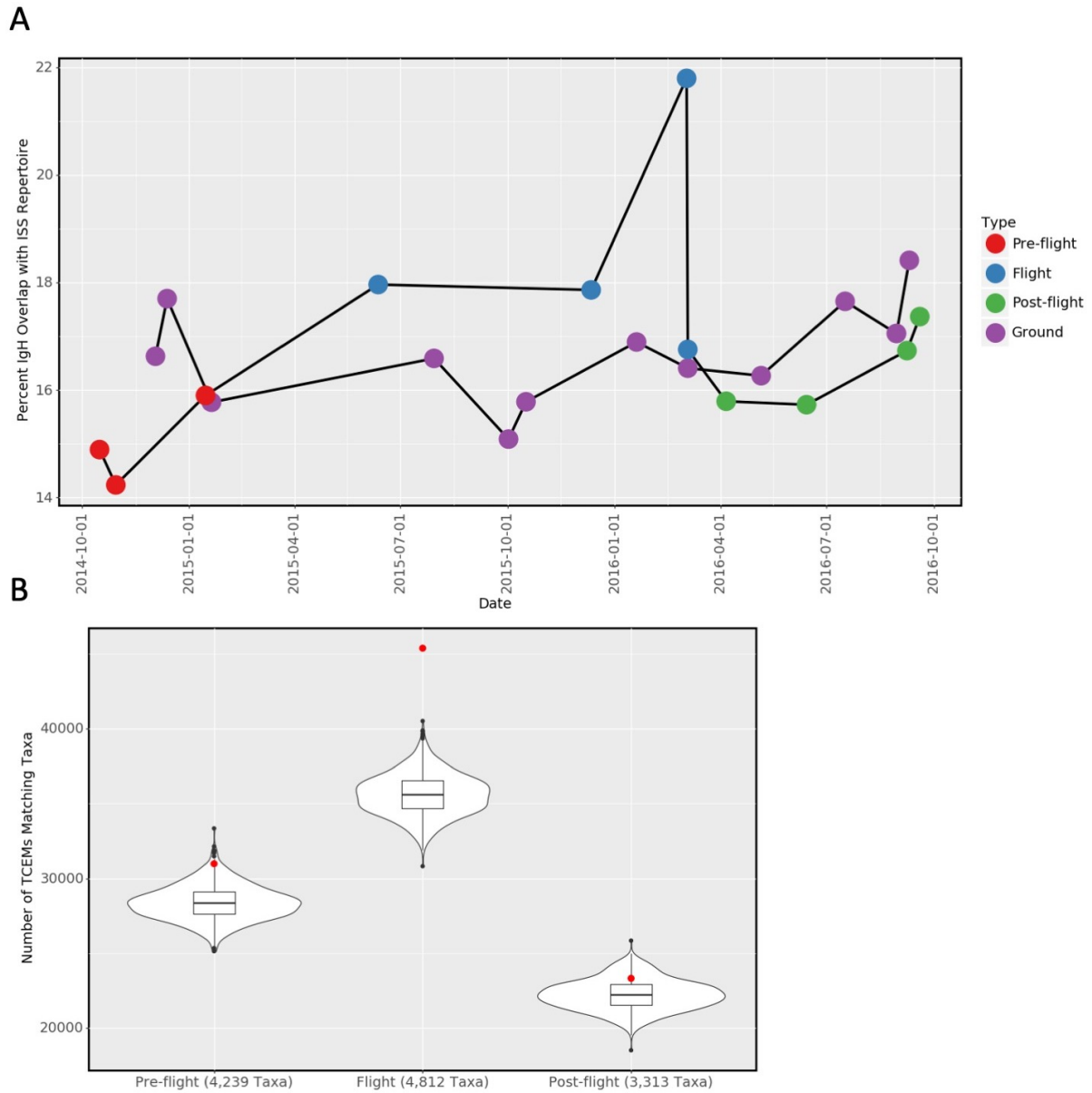


Figure 6: A) Overlap between TCEM repertoires and TCEM-targets found onboard the ISS. 'Ground' indicates HR. B) Number of TCEMs that match taxa found in both the ISS and flight (or pre and post-flight samples). The red dots indicate the actual values for each time point, the black distribution is made up of 10,000 random subsets of the same number of taxa for each time point. Many more TCEMs match ISS taxa from in-flight samples than pre-flight, post-flight, or random samples.

228 Note that the pooled repertoires were randomly subsampled to contain the same number of TCEMS.
229 We assessed how many taxa matching the TCEM repertoires were also found in the ISS: 4,812 matching
230 taxa were found from the in-flight repertoire compared to 4,239 for pre-flight and 3,313 for post-flight.

231 Finally, we counted the total number of matches between TCEMs and taxa which were found in the
232 ISS each time period (red dots in Figure 6B: with 45,373 found in flight, 30,982 for pre-flight, and 23,316
233 for post-flight). For comparison, we counted the number of matches found in 10,000 random subsets of
234 taxa for each time period, where the size of the subsets was the same as the number of ISS taxa matched
235 for each period. We found that the pre-flight taxa set had more matches than 9,856 random subsets
236 (empirical p-value = 0.0144) while post-flight had more matches than 8,527 random subsets ($p = 0.1473$).
237 However, the in-flight taxa set had far more matches than any tested random subset ($p < 0.0001$). This
238 is evidence that the match between TCEM repertoires in-flight and environmental targets in the ISS far
239 exceeds what would be expected by chance alone.

240 3 Conclusion

241 We have identified genetic and immunological evidence of microbial transfer between the fecal and saliva
242 microbiomes of an adult and between these microbiomes and their environment. These data, derived
243 from shotgun metagenomics sequencing and TCEMs, demonstrate that non-pathogenic microbes from
244 the environment can establish themselves in astronauts and suggests the possibility of ongoing microbial
245 flux between humans and the unique ISS environment. Moreover, these provide candidate "ISS mobile"
246 species and also enable a key estimate of the fraction of taxa that could be transferred from different
247 sources of the body while in the spaceflight environment.

248 A number of open questions remain. We have made a first attempt to quantify the rate of transfer
249 between different microbiomes and given an estimate for the total number of emergent species in a
250 gut microbiome, which cannot be explained as the result of repeated sampling alone. However, these
251 estimates necessarily suffer from the small sample sizes available in this study and the unusual situation
252 under which the samples were taken. To conclusively establish the scope of microbial transfer will
253 require broader studies targeting earth based environments, food varieties, and different communities,
254 as well as additional characterization using culture-based techniques. Nonetheless, the unusual nature of
255 spaceflight provides a strongly controlled environment, making this a near-optimal model for studying
256 microbial transfer.

257 The emergence of new taxa, while intriguing, must be placed into the context of expected stool
258 sampling variation. To account for such sampling dynamics, we also conducted a rigorous re-sampling
259 study. Our data showed that TW and HR had more newly observed taxa at some (but not all) of the
260 time points relative to the 100,000 subset. Importantly, the number of new taxa that were observed in
261 subsets dropped off quickly for later time points as the subsets reached saturation. Subsets generally
262 showed an adversarial selection, wherein many new taxa at one time point would lead to fewer new taxa
263 at later time points. The 243 fecal replicates had similar read counts to the time series from HR and
264 TW, reducing a source of potential bias, but could also be examined in greater detail in future studies.

265 Of note, repeated sampling can identify low abundance species which were dropped out of previous
266 samples and because different sample preparation techniques can yield different sets of taxa. A series
267 of samples taken from a microbiome that is exchanging taxa with an external environment will have
268 an additional source of new taxa. These taxa would not be identified in earlier samples because they
269 were not present, and this is another source of variation that could be mapped and quantified for future
270 missions (more sampling of more areas of the body and the ISS, and at greater depth).

271 The techniques for comparing immunological signatures in T-Cell repertoires to microbiomes are
272 nascent. To our knowledge, this is the first study to compare T-Cell repertoires and microbiomes in
273 humans using genetic data, but these techniques used may be limited in scope or accuracy. Though our
274 results suggest a shift of the T-Cell repertoire in response to the new and unique environment of the ISS,
275 we must temper this until these techniques can be proved and validated in other studies. Nonetheless,
276 such metrics can lay the foundation for a strong potential link between a person's T-cell dynamics and
277 their environment.

278 Taken together, the matching genomic regions across 16 taxa, the host immunological data, and
279 matching SNP haplotypes within the strains strongly supports the conclusion that novel taxa in pre-
280 flight commensal microbiomes from TW could come from the environment or from other commensal
281 microbiomes. The size of transferred regions and number of SNPs suggests that "taxa transfer" between
282 commensal microbiomes occurs more frequently than they transfer from the environment to commensal
283 microbiomes. However, these rates may prove to be anomalous for either TW, habitation in the ISS, or

284 both, since non-pathogenic microbial exchange with the environment represents a significant unknown
285 for its impact on human and astronaut health. Nevertheless, accurate quantification of microbial strains
286 and their movements can lead to targeted interventions, shed light on the hygiene hypothesis (broadly
287 and on the ISS), and help in planning for future missions and astronaut monitoring.

288 4 Availability and Access

289 All analysis and figure generating code may be found on GitHub at [https://github.com/dcdanko/
290 twins_iss_transfer](https://github.com/dcdanko/twins_iss_transfer). All results and raw data may be found on Pangea at [https://pangea.gimmbio.
291 com/sample-groups/62661efb-a433-4ae5-bcec-de704a80e217](https://pangea.gimmbio.com/sample-groups/62661efb-a433-4ae5-bcec-de704a80e217).

292 5 Author Contribution

293 DCD performed all bioinformatics analyses and defined the structure of the study with guidance from
294 CEM. NS led the collection of samples from the ISS. DJB and CM prepared samples for sequencing.
295 PJ, AK, MMC, GC, EA, coordinated sampling. FGB prepared samples for sequencing. SJG and MHV
296 handled sample coordination, sequencing, collection, analysis. KV led coordination with NASA and led
297 collection of samples on board the ISS. CEM led and conceived this study.

298 6 Acknowledgment

299 We would like to thank the Epigenomics Core Facility at Weill Cornell Medicine, the Scientific Comput-
300 ing Unit (SCU), XSEDE Supercomputing Resources, the Starr Cancer Consortium (I13-0052), the Vallee
301 Foundation, the WorldQuant Foundation, The Pershing Square Sohn Cancer Research Alliance, NASA
302 (NNX14AH50G, NNX17AB26G), the National Institutes of Health (R01AI151059), TRISH (NNX16AO69A:0107,
303 NNX16AO69A:0061), the Bill and Melinda Gates Foundation (OPP1151054), and the Alfred P. Sloan
304 Foundation (G-2015-13964).

305 Part of the research described in this article was carried out at the Jet Propulsion Laboratory,
306 California Institute of Technology, under a contract with NASA. This research was funded by 2012
307 Space Biology project NNH12ZTT001N grant 19-12829-26 under task order NNN13D111T awarded to
308 K.V., which also funded a postdoctoral fellowship for NKS.

309 7 Declaration of Interests

310 The authors declare they have no competing interests that impacted this study. CEM is co-founder of
311 Biotia and Onegevity.

312 8 Methods

313 8.1 Experimental setup and samples

314 We analyzed 18 fecal samples from two human subjects (9 each) and 42 environmental samples from the
315 ISS. All samples were assayed with 2x150bp DNA shotgun sequencing and analyzed as described below.
316 Exact sample handling and processing is described in the supplementary methods.

317 Human fecal samples were taken from two identical twins TW and HR both astronauts who had
318 previously been in space. During the study TW was sent on a roughly 1 year flight to the ISS while
319 HR remained on earth and functioned as a control. For many parts of this study samples from TW are
320 grouped into pre-flight, peri-flight, and post-flight groups. As much as practically possible samples from
321 HR were handled in an identical manner to samples from TW.

322 We note that the sampling of the ISS was initially planned and designed separately from the sampling
323 of the human subjects.

324 8.2 Sequencing

325 Samples from the human subject were extracted with a DNA extraction protocol adapted from the
326 Maxwell RSC Buccal Swab DNA kit (Catalogue number AS1640: Promega Corporation, Madison WI).

327 Briefly, 300 μ l of lysis buffer and 30 μ l of Proteinase K was mixed and added to each swab tube. Swab
328 tubes were then incubated for 20 min at 56 C using a Thermo Fisher water bath, removed from the
329 tubes, and fluid was transferred to well 1 of the Maxwell RSC Cartridge. The swab head was centrifuged
330 using a ClickFit Microtube (Cat. # V4741), and extracted fluid was added to the corresponding well of
331 Maxwell Cartridge, and eluted in 50 μ l of provided elution buffer.

332 Extracted DNA was taken forward to the Nextera Flex protocol by Illumina. Briefly, 30 μ l of extracted
333 DNA was taken into library prep protocol and run with 12 cycles of PCR. Libraries were cleaned up with
334 a left sided size selection, using a bead ratio of 0.8x. The right sided size selection was omitted. Libraries
335 were then quantified using a Thermo Fisher Qubit Fluorometer and an Advanced Analytical Fragment
336 Analyzer. Libraries were sequenced on an Illumina HiSeqPE 50 \times 2 at the Weill Cornell Epigenomics
337 Core.

338 Samples from the ISS were sequenced according to the protocol described in [Singh et al. \(2018\)](#).

339 8.3 Processing Short Read Sequencing Data

340 **Preprocessing and Taxonomic Profiling** We processed raw reads from all samples into taxonomic
341 profiles for each sample using the MetaSUB Core Analysis Pipeline ([Danko and Mason, 2020](#)). This
342 includes a preprocessing stage that consists of AdapterRemoval ([Schubert et al., 2016](#)), Human se-
343 quence removal with Bowtie2 ([Langmead and Steven L Salzberg, 2013](#)), and read error correction using
344 BayesHammer ([Nikolenko et al., 2013](#)). Subsequently reads were assigned to taxonomic groups using
345 Kraken2 ([Wood et al., 2019](#)). We generated a table of read counts giving the number of reads assigned
346 to each species for each sample.

347 **Identification of candidate species for strain level analysis** We analyzed our table of species level
348 read counts to identify candidate lists of *transient* and *persistent* transfer species. We held a transient
349 species to be one that was transferred from the ISS into the astronaut only while the astronaut remained
350 in the ISS and which was be cleared after return to earth. We held persistent species to be those that
351 were transferred from the ISS to the astronaut which remained after return to earth.

352 We statistically analyzed our table of read counts using Aldex2 ([Fernandes et al., 2013](#)). Remaining
353 samples (from astronauts) were split into two groups. The first group was the control group and consisted
354 of all samples from TW before flight and all samples from HR at any point. The second group was the
355 case group and consisted of all samples from TW during flight. Samples from TW after flight were
356 assigned to the control group for analysis of transients and to the case group for analysis of persistents.
357 Aldex2 was used to identify differentially abundant taxa between the two groups. We selected all taxa
358 that were significantly ($q < 0.05$ by Welch's t-test with Benjamini Hochberg correction) more abundant
359 in the case group than in the control group. We then filtered these two list (persistent and transient) to
360 include only species found in the ISS samples (minimum 10 reads in 25% of samples).

361 **Strain Analysis** Reads were further processed for strain level analysis using the MetaSUB Core Anal-
362 ysis Pipeline. Given a specified organism to examine we downloaded all available reference genomes from
363 RefSeq. If more than 100 reference genomes were available we selected 100 at random. Human-depleted
364 reads were mapped to each genome using Bowtie2 (sensitive presets) and pileup files were generated
365 using from alignments using samtools ([Li et al., 2009](#)). Pileups were analyzed for coverage patterns using
366 purpose built code (see availability for access). SNPs were identified by comparing aligned bases from
367 short reads to reference sequences, SNP filtering was performed as part of identifying co-stranded SNPs.

368 **Identifying co-stranded SNPs** We developed a technique to identify SNPs that occurred on the
369 same genetic strand. The technique is, in practice, limited to identifying co-stranded SNPs within 1kbp
370 of on another. The technique works by formulating SNP recovery as an instance of the multi-community
371 recovery problem. We start by building a graph of SNPs. Each SNP forms a node in the graph and is
372 identified by its genomic position and base. Edges are added between SNPs that are found on the same
373 read. Edges are undirected but weighted by the number of times a pair of SNPs is found on the same
374 read. The SNP graph is then filtered to remove SNPs that occur only once as these are likely to be
375 errors and are uninformative in any case. The remaining graph is clustered into groups of SNPs using
376 the approach to the multi-community recovery problem by [Blondel et al. \(2008\)](#). The final result of this
377 are sets of SNPs that are often found on the same read.

378 This technique is similar to techniques used for phasing SNPs to one strand of a diploid genome such
379 as [Zheng et al. \(2016\)](#). The key difference between this technique and ours is that there may be more
380 than two communities in our case and that we make only attempt to cluster proximal SNPs.

381 8.4 Analyzing Human and Environmental Immune Repertoires

382 **Sample collection, preparation, and sequencing** Samples were collected and sequenced according
383 to the protocol described in [Garrett-Bakelman et al. \(2019b\)](#). Briefly, PBMCs were flow sorted for
384 CD4+ t-cells. RNA from these CD4+ T-Cells was selected using Poly-A pulldown leaving, largely, only
385 RNA that would be translated and depleting ribosomal RNA. PolyA selected RNA was sequenced using
386 Illumina machines for 2x150bp reads.

387 **Assembling Immunoglobulin Heavy (IgH) sequences from short reads** We used MiXCR
388 (v3.0.13) to build IgH sequences from poly-a selected RNA taken from CD4+ t-cells ([Monk et al., 2017](#)).
389 We used the recommended workflow for non-specific RNA sequences and selected for IGH sequences
390 using the built in export tool. The precise commands used are recorded in the attached `run_mixcr.py`
391 file.

392 **Creating a repertoire of t-cell exposed motifs (TCEMs) from IgH sequences** We assembled
393 a repertoire of TCEMs from our IgH sequences following the method described by [Breme and Homan](#)
394 ([2015](#)). Briefly, this method consists of taking 5 amino acid (aa) sub-sequences from IgH sequences.
395 The 5aa sequences are found according to three specific spaced patterns within larger windows of 9, 15,
396 and 15 amino acids respectively. These patterns are meant to reflect binding potential within the MHC
397 groove. TCEM sequences are found by iterating every possible window (of both sizes) along the length
398 of an IgH sequence and generating a 5aa sequence using the appropriate window. For a sample (or set
399 of samples) we generated a full TCEM repertoire by concatenating the repertoire for each IgH sequence.
400 For reference we note that there are only $20^5 = 3.2 * 10^6$ possible 5aa sequences so significant overlap is
401 possible between even randomly generated sets.

402 **Creating a repertoire of TCEM targets from metagenomic data** We generated sets of potential
403 amino acid sequences that could match our TCEM sequences from metagenomic data. We counted all
404 canonical 15 base pair nucleotide sequences from pre-processed and error corrected (see above) reads
405 using Jellyfish ([Marçais and Kingsford, 2011](#)). We translated all resulting 15-mers and their reverse
406 complement using the standard codon to aa table and discarded any aa sequence that contained a stop
407 codon. Count information was retained for aa sequences from jellyfish. Any 5aa sequence that occurred
408 with a frequency of less than 1 part per million was discarded.

409 **Comparing metagenomic and t-cell repertoires** We compared the number of 5aa sequences
410 which were found in both our metagenomic data and IgH sequences. Even with abundance filtering
411 metagenomes typically still contained many more sequences than IgH repertoires. To assess overlap
412 between an IgH repertoire and a metagenome we took the number of 5aa sequences from the IgH
413 repertoire which were also found in the metagenome divided by the total number of 5aa sequences in the
414 IgH repertoire.

415 **Identifying potential taxonomic matches to TCEM repertoires** We identified potential tax-
416 onomic matches to 5aa TCEM sequences by aligning them to the NCBI NR protein database using
417 BLASTp. We accepted all 100% identity matches that included a taxonomic label. Since 5aa sequences
418 are too short to be specific to one taxa there were typically multiple taxa for each TCEM. For a repertoire
419 of TCEMs we built a binary matrix of TCEM sequences and taxa, each element in this matrix was set to
420 true if and only if the given TCEM was found in the given taxon. This enabled us to generate statistics
421 such as the number of TCEMs which could potentially match a taxon or the number of taxons for each
422 TCEM.

423 References

424 Blondel, V. D., Guillaume, J.-L., Lambiotte, R., and Lefebvre, E. (2008). Fast unfolding of communities
425 in large networks. *Journal of Statistical Mechanics: Theory and Experiment*, 2008(10):P10008.

- 426 Breme, R. D. and Homan, E. J. (2015). Extensive T-cell epitope repertoire sharing among human
427 proteome, gastrointestinal microbiome, and pathogenic bacteria: Implications for the definition of self.
428 *Frontiers in Immunology*, 6(OCT).
- 429 Danko, D., Bezdán, D., Afshinnekoo, E., Ahsanuddin, S., Bhattacharya, C., Butler, D. J., Chng, K. R.,
430 De Filippis, F., Hecht, J., Kahles, A., et al. (2019). Global genetic cartography of urban metagenomes
431 and anti-microbial resistance. *BioRxiv*, page 724526.
- 432 Danko, D. C. and Mason, C. (2020). The metasub microbiome core analysis pipeline enables large scale
433 metagenomic analysis.
- 434 Fernandes, A. D., Macklaim, J. M., Linn, T. G., Reid, G., and Gloor, G. B. (2013). ANOVA-Like
435 Differential Expression (ALDEx) Analysis for Mixed Population RNA-Seq. *PLoS ONE*, 8(7).
- 436 Garrett-Bakelman, F. E., Darshi, M., Green, S. J., Gur, R. C., Lin, L., Macias, B. R., McKenna, M. J.,
437 Meydan, C., Mishra, T., Nasrini, J., et al. (2019a). The nasa twins study: A multidimensional analysis
438 of a year-long human spaceflight. *Science*, 364(6436).
- 439 Garrett-Bakelman, F. E., Darshi, M., Green, S. J., Gur, R. C., Lin, L., Macias, B. R., McKenna, M. J.,
440 Meydan, C., Mishra, T., Nasrini, J., Piening, B. D., Rizzardi, L. F., Sharma, K., Siamwala, J. H.,
441 Taylor, L., Vitaterna, M. H., Afkarian, M., Afshinnekoo, E., Ahadi, S., Ambati, A., Arya, M., Bezdán,
442 D., Callahan, C. M., Chen, S., Choi, A. M., Chlipala, G. E., Contrepois, K., Covington, M., Crucian,
443 B. E., De Vivo, I., Dinges, D. F., Ebert, D. J., Feinberg, J. I., Gandara, J. A., George, K. A., Goutsias,
444 J., Grills, G. S., Hargens, A. R., Heer, M., Hillary, R. P., Hoofnagle, A. N., Hook, V. Y., Jenkinson,
445 G., Jiang, P., Keshavarzian, A., Laurie, S. S., Lee-McMullen, B., Lumpkins, S. B., MacKay, M.,
446 Maienschein-Cline, M. G., Melnick, A. M., Moore, T. M., Nakahira, K., Patel, H. H., Pietrzyk, R.,
447 Rao, V., Saito, R., Salins, D. N., Schilling, J. M., Sears, D. D., Sheridan, C. K., Stenger, M. B.,
448 Tryggvadottir, R., Urban, A. E., Vaisar, T., Van Espen, B., Zhang, J., Ziegler, M. G., Zwart, S. R.,
449 Charles, J. B., Kundrot, C. E., Scott, G. B., Bailey, S. M., Basner, M., Feinberg, A. P., Lee, S. M.,
450 Mason, C. E., Mignot, E., Rana, B. K., Smith, S. M., Snyder, M. P., and Turek, F. W. (2019b). The
451 NASA twins study: A multidimensional analysis of a year-long human spaceflight. *Science*, 364(6436).
- 452 Goodrich, J. K., Davenport, E. R., Beaumont, M., Jackson, M. A., Knight, R., Ober, C., Spector, T. D.,
453 Bell, J. T., Clark, A. G., and Ley, R. E. (2016). Genetic Determinants of the Gut Microbiome in UK
454 Twins. *Cell Host and Microbe*, 19(5):731–743.
- 455 Langmead and Steven L Salzberg (2013). Bowtie2. *Nature methods*, 9(4):357–359.
- 456 Li, H., Handsaker, B., Wysoker, A., Fennell, T., Ruan, J., Homer, N., Marth, G., Abecasis, G., and
457 Durbin, R. (2009). The Sequence Alignment/Map format and SAMtools. *Bioinformatics*, 25(16):2078–
458 2079.
- 459 Marçais, G. and Kingsford, C. (2011). A fast, lock-free approach for efficient parallel counting of occur-
460 rences of k-mers. *Bioinformatics*, 27(6):764–770.
- 461 Monk, J. M., Lloyd, C. J., Brunk, E., Mih, N., Sastry, A., King, Z., Takeuchi, R., Nomura, W., Zhang,
462 Z., Mori, H., Feist, A. M., and Palsson, B. (2017). Antigen receptor repertoire profiling from RNA-seq
463 data.
- 464 Nicolaou, N., Siddique, N., and Custovic, A. (2005). Allergic disease in urban and rural populations:
465 Increasing prevalence with increasing urbanization. *Allergy: European Journal of Allergy and Clinical
466 Immunology*, 60(11):1357–1360.
- 467 Nikolenko, S. I., Korobeynikov, A. I., and Alekseyev, M. A. (2013). BayesHammer: Bayesian clustering
468 for error correction in single-cell sequencing. *BMC Genomics*, 14.
- 469 Root-Bernstein, R. (2016). Autoimmunity and the microbiome: T-cell receptor mimicry of “self” and
470 microbial antigens mediates self tolerance in holobionts. *BioEssays*, 38(11):1068–1083.
- 471 Sasada, R., Weinstein, M., Danko, D., Wolfe, E., Tang, S., Jarvis, K., Grim, C., Lagishetty, V., Jacobs,
472 J., Arnold, J., Kemp, R., and Mason, C. (2020). Progress Towards Standardizing Metagenomics:
473 Applying Metagenomic Reference Material to Develop Reproducible Microbial Lysis Methods with
474 Minimum Bias. *Journal of biomolecular techniques : JBT*, 31:S30–S31.

- 475 Schubert, M., Lindgreen, S., and Orlando, L. (2016). AdapterRemoval v2: rapid adapter trimming,
476 identification, and read merging. *BMC Research Notes*, 9(1):88.
- 477 Schwendner, P., Mahnert, A., Koskinen, K., Moissl-Eichinger, C., Barczyk, S., Wirth, R., Berg, G., and
478 Rettberg, P. (2017). Preparing for the crewed Mars journey: microbiota dynamics in the confined
479 Mars500 habitat during simulated Mars flight and landing. *Microbiome*, 5(1):129.
- 480 Singh, N. K., Wood, J. M., Karouia, F., and Venkateswaran, K. (2018). Succession and persistence of
481 microbial communities and antimicrobial resistance genes associated with International Space Station
482 environmental surfaces. *Microbiome*, 6(1).
- 483 Wood, D. E., Lu, J., and Langmead, B. (2019). Improved metagenomic analysis with Kraken 2. *Genome*
484 *Biology*, 20(1).
- 485 Zheng, G. X., Lau, B. T., Schnall-Levin, M., Jarosz, M., Bell, J. M., Hindson, C. M., Kyriazopoulou-
486 Panagiotopoulou, S., Masquelier, D. A., Merrill, L., Terry, J. M., Mudivarti, P. A., Wyatt, P. W.,
487 Bharadwaj, R., Makarewicz, A. J., Li, Y., Belgrader, P., Price, A. D., Lowe, A. J., Marks, P., Vurens,
488 G. M., Hardenbol, P., Montesclaros, L., Luo, M., Greenfield, L., Wong, A., Birch, D. E., Short, S. W.,
489 Bjornson, K. P., Patel, P., Hopmans, E. S., Wood, C., Kaur, S., Lockwood, G. K., Stafford, D.,
490 Delaney, J. P., Wu, I., Ordonez, H. S., Grimes, S. M., Greer, S., Lee, J. Y., Belhocine, K., Giorda,
491 K. M., Heaton, W. H., McDermott, G. P., Bent, Z. W., Meschi, F., Kondov, N. O., Wilson, R.,
492 Bernate, J. A., Gauby, S., Kindwall, A., Bermejo, C., Fehr, A. N., Chan, A., Saxonov, S., Ness, K. D.,
493 Hindson, B. J., and Ji, H. P. (2016). Haplotyping germline and cancer genomes with high-throughput
494 linked-read sequencing. *Nature Biotechnology*, 34(3):303–311.

495 Supplement

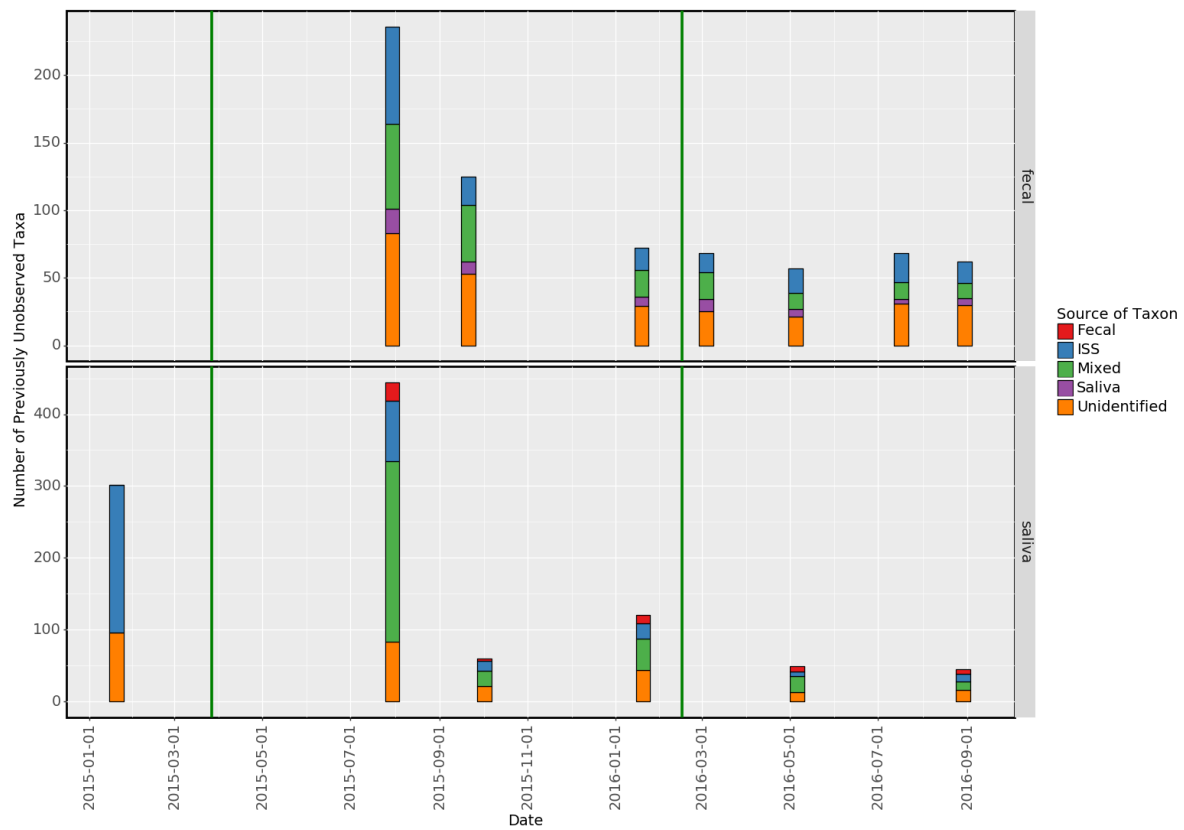


Figure S1: This plot shows the number of taxa at each time point that were not observed at any previous timepoint for fecal and saliva samples from HR. The colors indicate the likely source of the new taxon if it was found previously in the saliva (for fecal samples, vice versa for saliva samples), the ISS, both (Mixed), or neither.

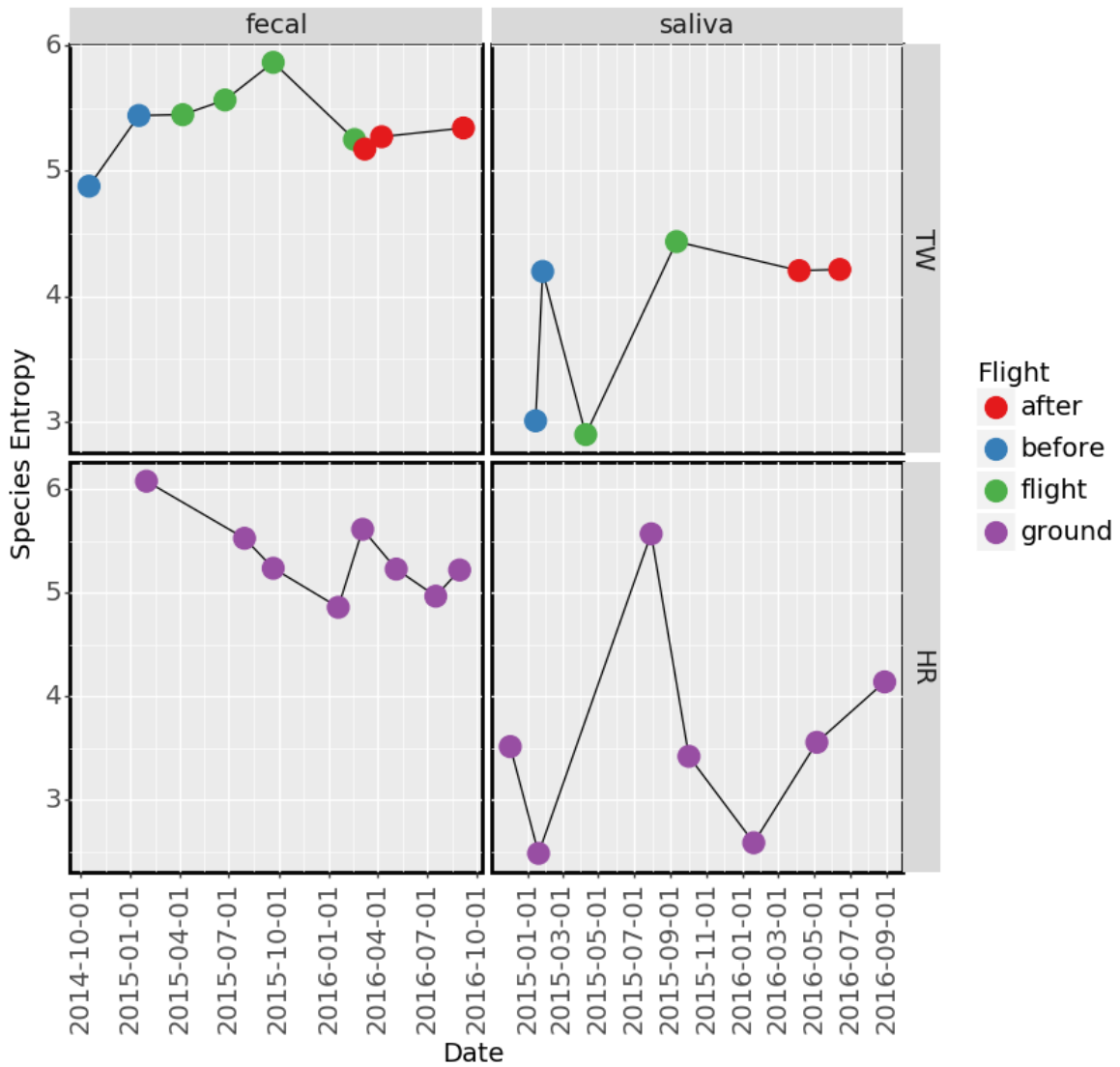


Figure S2: Vertical shows species entropy (Shannon entropy of species relative abundances) for sample types in both twins.

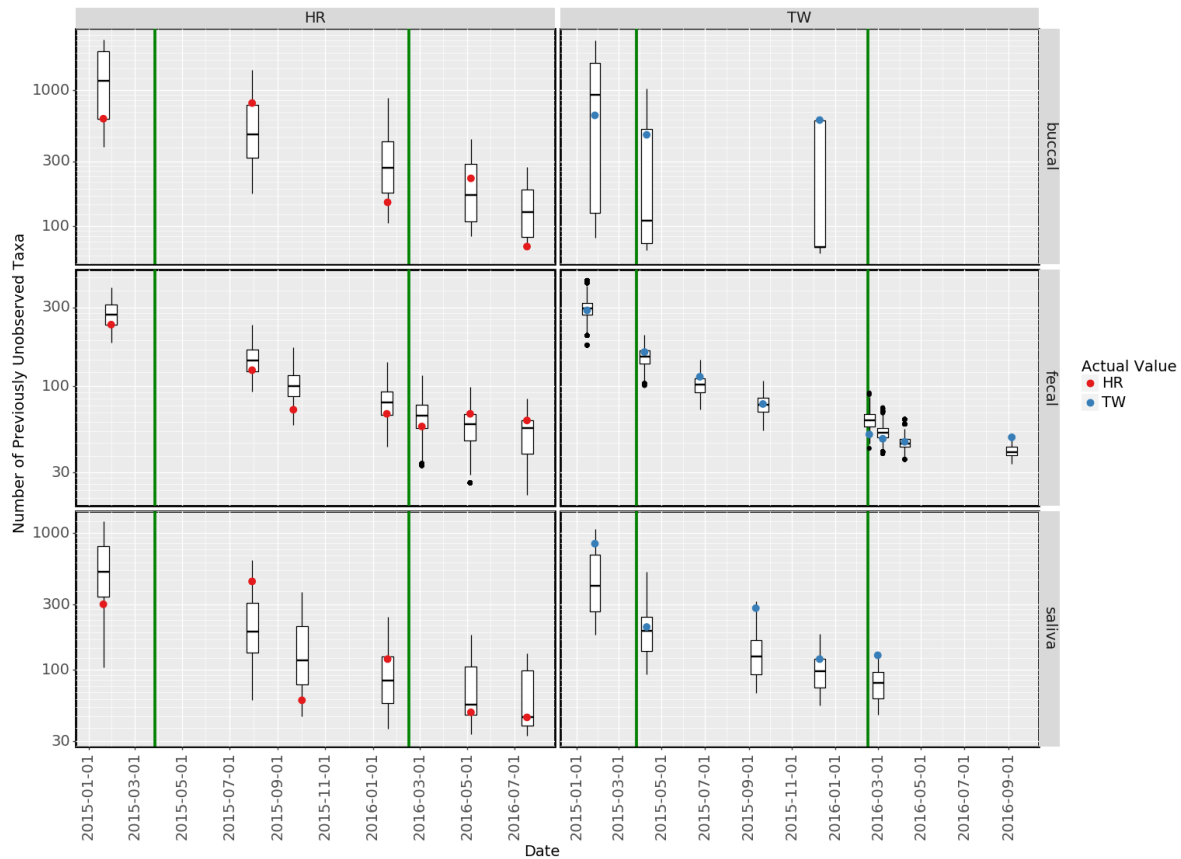


Figure S3: This plot shows the number of taxa at each time point that were not observed at any previous timepoint. The first timepoint is omitted from the plot since no taxa had been previously observed. Boxplots indicate an artificial reference distribution generated by randomly permuting timestamps. Red and blue dots indicate actual values.

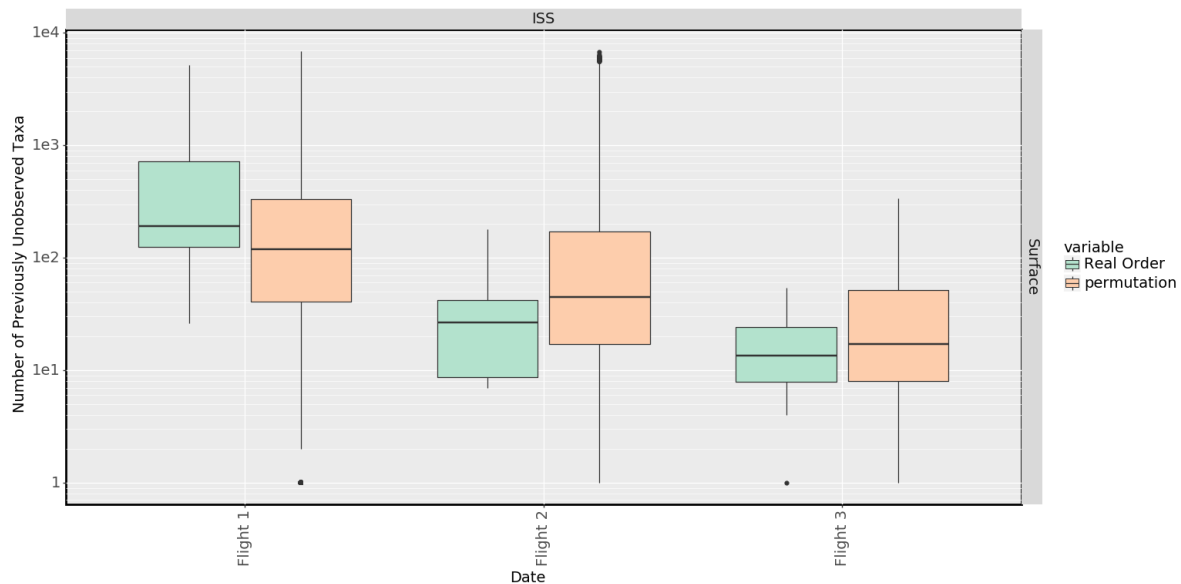


Figure S4: This plot shows the number of taxa at each time point that were not observed at any previous time point for the ISS. ISS samples are grouped into 'flights' where each sample in the same flight was taken on the same day. One sample from flight 1 is arbitrarily chose as the 'first' sample and used as the comparison. Boxplots indicate the real distribution of new taxa as well as an artificial reference distribution generated by randomly permuting timestamps.

Table 2: Size of regions that may have been transferred in kilobases. Gut-Saliva transfer means that a region was found in either the gut or saliva microbiome pre-flight, then found in the other during-flight. Environment transfer means a region was not found in either fecal or saliva microbiomes from TW pre-flight but was found during flight and was also present in the ISS.

	Pre-flight	Gut-Saliva transfer	Environment transfer
<i>Bifidobacterium pseudocatenulatum</i>	243.9	92.4	85.2
<i>Brevibacterium siliguriense</i>	18.7	2.6	3.1
<i>Gordonibacter urolithinfaciens</i>	37.8	12.9	21.2
<i>Bacillus albus</i>	87.6	7.0	14.1
<i>Gluconobacter albidus</i>	10.2	2.5	1.3
<i>Fusobacterium necrophorum</i>	86.4	18.0	56.8
<i>Geobacillus stearothermophilus</i>	73.5	13.7	13.8
<i>Bifidobacterium catenulatum</i>	258.8	17.5	40.3
<i>Streptococcus viridans</i>	2319.6	92.9	221.8
<i>Vibrio alginolyticus</i>	211.0	10.6	89.7
<i>Staphylococcus sciuri</i>	179.0	19.4	37.4
<i>Pectobacterium parmentieri</i>	269.0	22.7	56.7
<i>Campylobacter lari</i>	42.0	8.7	18.1
<i>Atlantibacter hermannii</i>	66.4	15.7	30.6
<i>Bacillus tequilensis</i>	57.4	6.0	8.7
<i>Achromobacter ruhlandii</i>	49.8	13.6	11.7
<i>Serratia proteamaculans</i>	70.0	11.2	6.7
<i>Leptotrichia hongkongensis</i>	115.2	0.7	21.5
<i>Exiguobacterium antarcticum</i>	21.5	4.4	6.2
<i>Anoxybacillus amylolyticus</i>	11.5	2.2	2.3
<i>Kosakonia sacchari</i>	65.4	16.0	30.8
<i>Yersinia canariae</i>	18.2	8.2	7.7
<i>Providencia heimbachae</i>	76.0	12.1	6.5
<i>Spirochaeta perfilievii</i>	2.7	0.4	0.7
<i>Cronobacter condimenti</i>	15.2	8.5	18.8
<i>Brenneria rubrifaciens</i>	13.2	5.7	7.3
<i>Staphylococcus simiae</i>	20.8	1.5	6.2

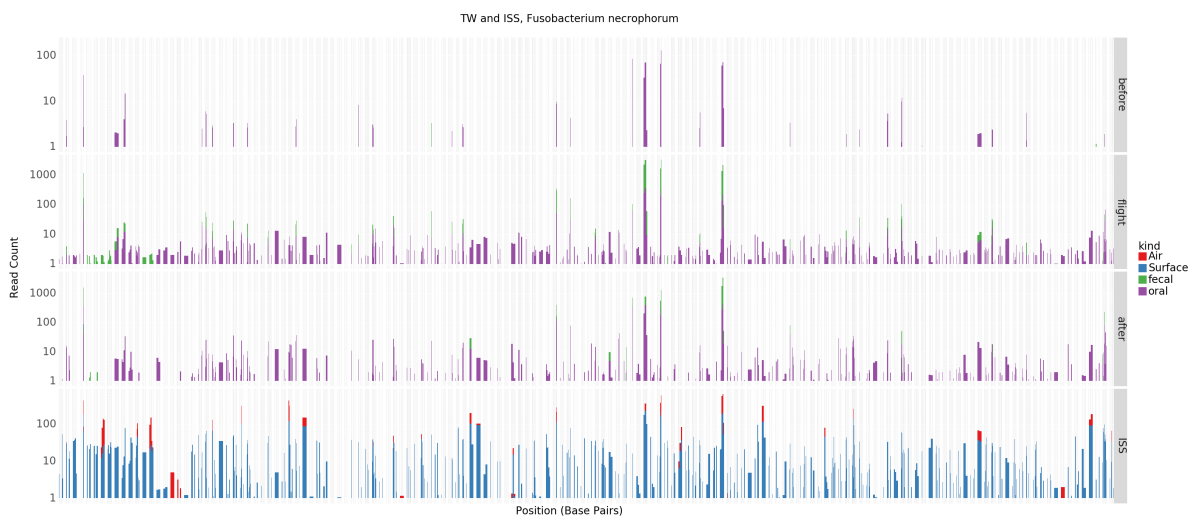


Figure S5: Rows show consolidated samples from before, during and after flight (or from the ISS at any point) from TW. Columns represent all available contigs for taxon. Colored bars represent 100bp covered, on average, at the specified read depth. A number of contigs are only covered in TW during and after flight.

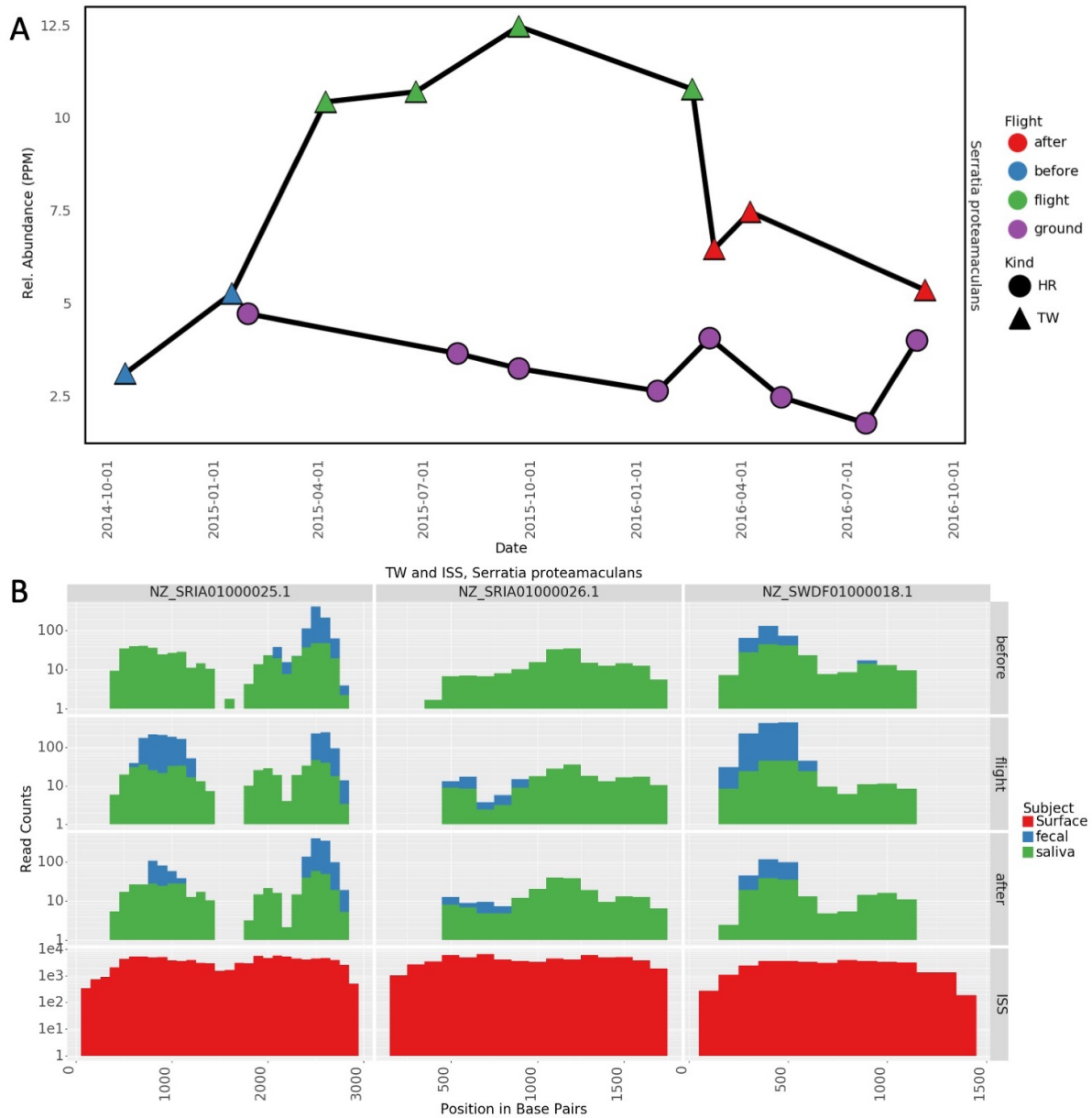


Figure S6: A) Relative abundance of *Serratia proteamaculans* in fecal samples from TW and HR. Relative abundance is given in units of parts per million. B) Coverage of candidate persistent transfer regions of the *Serratia proteamaculans* genome.

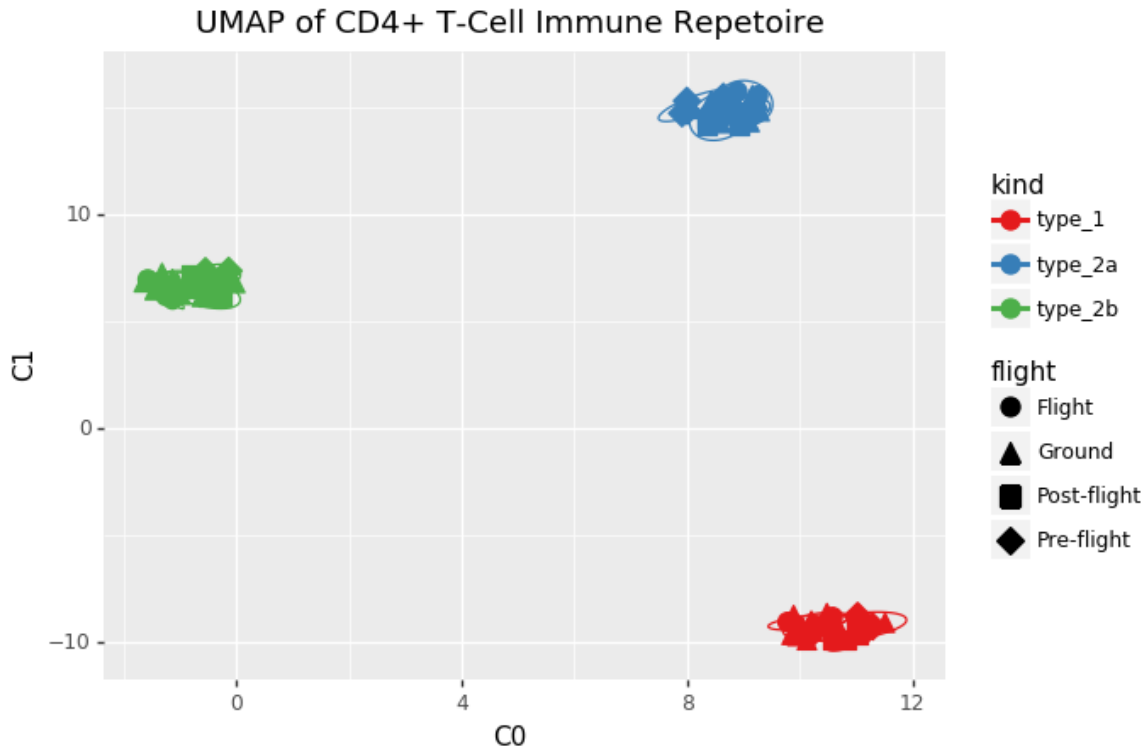


Figure S7: UMAP plot of similarity between TCEM repertoires of all types. 'Ground' indicates HR.

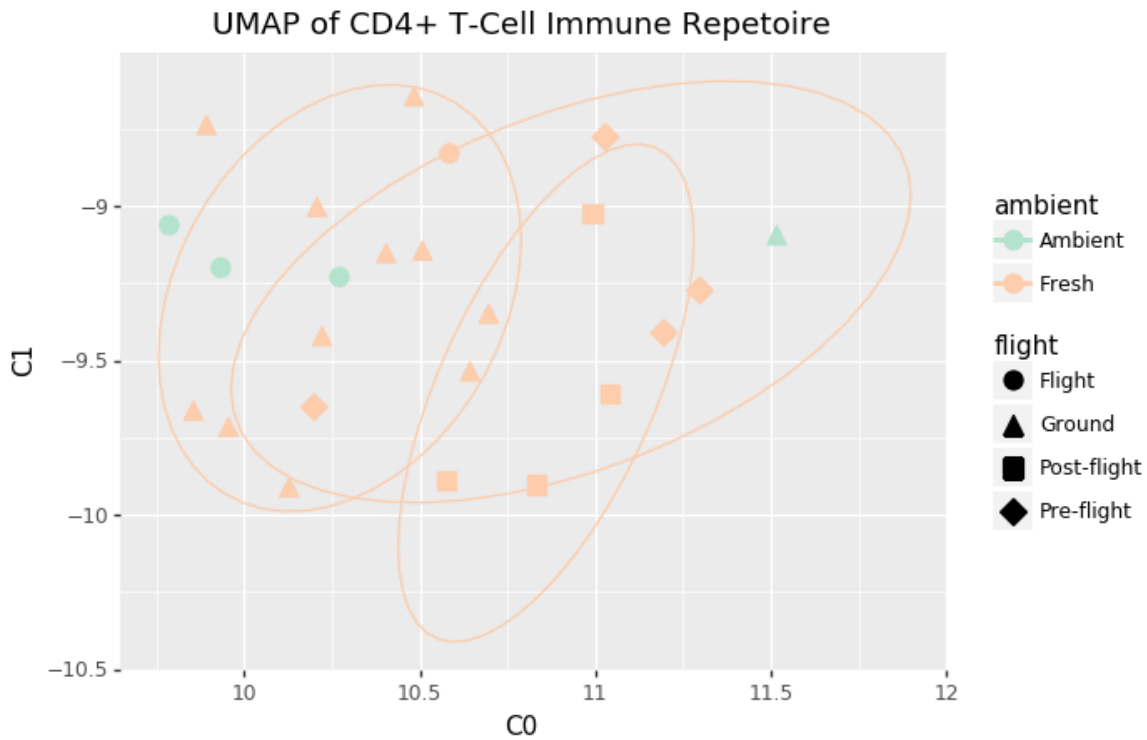


Figure S8: UMAP plot of similarity between type 1 TCEM repertoires of all types. Color shows method of return

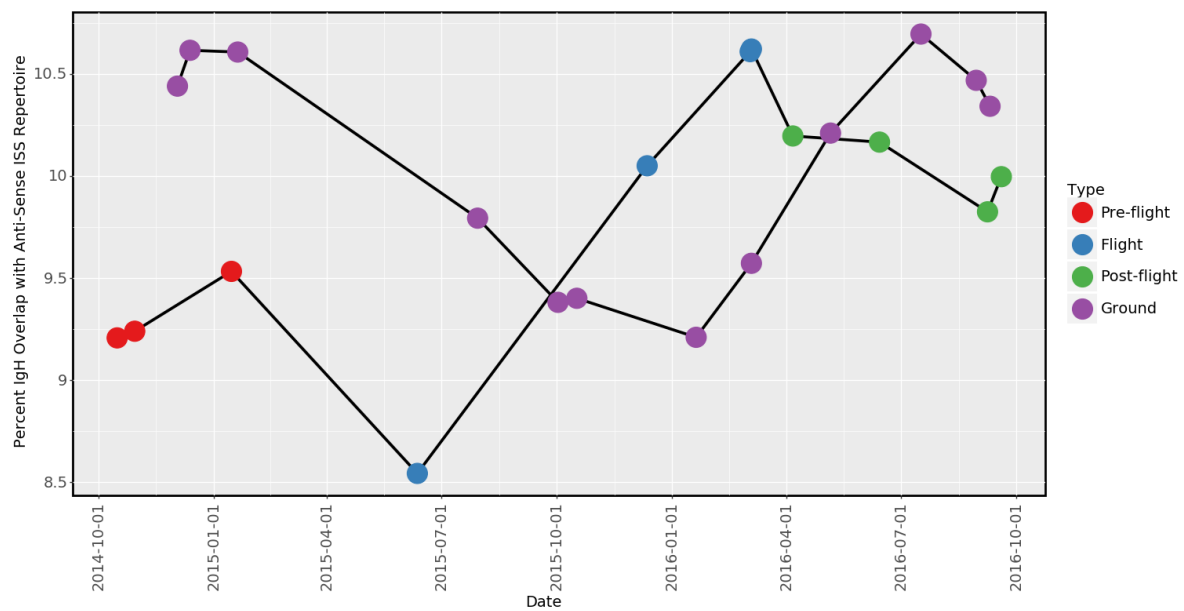


Figure S9: Overlap between anti-sense TCEM repertoires and regular TCEM-targets found on board the ISS. 'Ground' indicates HR. Anti-sense proteins are not expected to match, this serves as a negative control test.